

Ordering of oxygen moments in ferromagnetic edge-sharing CuO_4 chains in $\text{La}_{14-x}\text{Ca}_x\text{Cu}_{24}\text{O}_{41}$

M. Matsuda

The Institute of Physical and Chemical Research (RIKEN), Wako, Saitama 351-01, Japan

K. M. Kojima and Y. J. Uemura

Department of Physics, Columbia University, New York, New York 10027

J. L. Zarestky

Ames Laboratory, Ames, Iowa 50011

K. Nakajima and K. Kakurai

Neutron Scattering Laboratory, ISSP, The University of Tokyo, Tokai, Ibaraki 319-11, Japan

T. Yokoo,* S. M. Shapiro, and G. Shirane

Department of Physics, Brookhaven National Laboratory, Upton, New York 11973

(Received 5 November 1997)

Neutron scattering measurements have been performed on the $S = \frac{1}{2}$ quasi-one-dimensional system $\text{La}_5\text{Ca}_9\text{Cu}_{24}\text{O}_{41}$, which consists of edge-sharing CuO_4 chains. We observed that the chains show an antiferromagnetic long-range ordering below $T_N = 10.5$ K with ferromagnetic correlations within the chain. In the antiferromagnetically ordered phase, an ordering of oxygen moments ($\sim 0.02\mu_B$) as well as that of Cu moments ($\sim 0.2\mu_B$) is observed. The oxygen moments are coupled with Cu moments ferromagnetically. [S0163-1829(98)03218-4]

I. INTRODUCTION

Spin- $\frac{1}{2}$ one-dimensional (1D) magnets show novel phenomena originating from quantum fluctuations. As a by-product of the high-temperature superconducting copper oxides, many interesting quasi-1D copper oxides have been discovered or rediscovered and have been studied intensively. The copper oxides such as Sr_2CuO_3 and Ca_2CuO_3 have chains of corner-sharing CuO_4 tetragons, in which copper spins are coupled by the nearly 180° Cu-O-Cu interaction. Since the ratio between intrachain (J) and interchain interactions (J') of the compounds is very large ($J/J' \sim 10^3$), they are thought of as ideal examples of the spin- $\frac{1}{2}$ 1D Heisenberg antiferromagnets.^{1,2} On the other hand, the copper oxides with chains of edge-sharing CuO_4 tetragons, in which copper spins are coupled by the nearly 90° Cu-O-Cu interaction, exhibit various interesting phenomena. The interaction depends sensitively on the bond angle θ between copper and oxygen ions and changes from ferromagnetic ($\theta < \sim 95^\circ$) to antiferromagnetic ($\theta > \sim 95^\circ$).³ The edge-sharing CuO_4 chains in CuGeO_3 have antiferromagnetic interaction and show a spin-Peierls transition at low temperature.⁴ In Li_2CuO_2 the interaction within the chains is ferromagnetic and an antiferromagnetic transition occurs at 9.3 K due to the fairly large antiferromagnetic interchain interaction.⁵ The chains in $\text{Sr}_{14}\text{Cu}_{24}\text{O}_{41}$ show a dimerized state which has longer-ranged spin correlations.^{6,7} The dimerized state is closely related with localized holes which exist at oxygen sites.

The magnetic properties of $\text{La}_6\text{Ca}_8\text{Cu}_{24}\text{O}_{41}$, which has both chains of edge-sharing CuO_4 tetragons and two-leg ladders of coppers,⁸ have been studied.^{9,10} $\text{La}_6\text{Ca}_8\text{Cu}_{24}\text{O}_{41}$ has a long-range magnetic order below 12.2 K in the chain while

the two-leg ladder remains singlet down to at least 4 K. The Cu spins are aligned ferromagnetically along the chain (c axis) with antiferromagnetic correlations between nearest-neighbor chains along the b axis. The spins have a spiral structure along the a axis with a rotation angle of $\sim 2\pi/5$.¹⁰ However, the exact spin structure was unknown due to the complicated diffraction pattern. Especially puzzling is a modulation of the intensity along the h direction, which shows a maximum around $h = 2.5$. One possibility to explain the scattered intensities would be that the Cu spins are tilted from the b axis. To confirm the model, polarized neutron experiments were performed.¹¹ No distinct scattering was observed in the vertical field (along the b axis) spin-flip mode experiments, which indicates that a spin component perpendicular to the b axis is negligible. This is inconsistent with the tilted spin model mentioned above. Further experiments discussed below were performed to solve this puzzle.

The interesting feature of $\text{La}_{14-x}\text{Ca}_x\text{Cu}_{24}\text{O}_{41}$ is that holes can be doped in the chain. It is expected that the holes are localized at oxygen sites and couple with the copper spins to form the Zhang-Rice singlet. In order to understand the spin structure of $\text{La}_6\text{Ca}_8\text{Cu}_{24}\text{O}_{41}$ in detail we study how the magnetic structure is changed with hole-doping. Neutron scattering measurements are performed on $\text{La}_5\text{Ca}_9\text{Cu}_{24}\text{O}_{41}$ in which holes are slightly introduced. The number of holes in the chain can be estimated as 4.2%, if one assumes that all the holes exist in the chain. The experiments show that $\text{La}_5\text{Ca}_9\text{Cu}_{24}\text{O}_{41}$ has an antiferromagnetic long-range ordering below $T_N = 10.5$ K with ferromagnetic correlations within the chain. Unlike $\text{La}_6\text{Ca}_8\text{Cu}_{24}\text{O}_{41}$, which shows an incommensurate structure along the a axis, $\text{La}_5\text{Ca}_9\text{Cu}_{24}\text{O}_{41}$ has a commensurate structure (antiferromagnetic correlations between nearest-neighbor chains along the a and b axes). Because of

the rather simple neutron diffraction pattern, a detailed magnetic structural analysis is possible. Unexpectedly, a polarization of oxygen moments is needed to explain the magnetic intensities in the antiferromagnetically ordered phase. The oxygen moments are coupled with copper moments ferromagnetically. To the best of our knowledge, this is the first observation of a polarization of oxygen moments in the copper oxide system. From these results the spin structure of $\text{La}_5\text{Ca}_9\text{Cu}_{24}\text{O}_{41}$ can also be determined.

II. EXPERIMENTAL DETAILS

The single crystal of $\text{La}_5\text{Ca}_9\text{Cu}_{24}\text{O}_{41}$ was grown using a traveling solvent floating zone (TSFZ) method at 3 bars oxygen atmosphere. The dimension of the cylindrically shaped crystal used in the experiments is about $5 \times 5 \times 20 \text{ mm}^3$. The effective mosaic of the single crystal is less than 0.4° with the spectrometer condition as described below. It is expected that La and Ca are distributed homogeneously in the sample since the lattice constant b systematically changes and the linewidth of the nuclear Bragg peaks does not change when the ratio of La and Ca is changed. The lattice constants of $\text{La}_5\text{Ca}_9\text{Cu}_{24}\text{O}_{41}$ are $a = 11.29 \text{ \AA}$, $b = 12.58 \text{ \AA}$, and $c = 27.61 \text{ \AA}$ at 1.7 K.

The neutron scattering experiments were carried out on the ISSP-PONTA spectrometer installed at the 5G beam hole of the Japan Research Reactor 3M (JRR-3M) at Japan Atomic Energy Research Institute (JAERI) and the HB3 triple-axis spectrometer at the High Flux Isotope Reactor (HFIR) at Oak Ridge National Laboratory (ORNL). The horizontal collimator sequences were open- $40'$ - S - $80'$ - $80'$ (unpolarized neutron) and open- $80'$ - S - $80'$ - $80'$ (polarized neutron) for the experiments on the ISSP-PONTA and open- $40'$ - S - $60'$ - $120'$ for the unpolarized neutron experiments on the HB3. The incident neutron energy was fixed at $E_i = 14.7 \text{ meV}$. Pyrolytic graphite (002) was used as monochromator and analyzer for unpolarized neutron experiments. Heusler alloy (111) was used as monochromator and analyzer for polarized neutron experiments. A flipping ratio of ~ 35 was measured on some nuclear Bragg peaks, corresponding to 94% polarization of the beam. Contamination from higher-order beam was effectively eliminated using pyrolytic graphite filters before and after the sample. The single crystals were mounted in a ^4He pumped cryostat which allowed us to perform the measurements down to 1.5 K. The crystals were oriented in the $(h,0,l)$ or $(0,k,l)$ scattering planes. As described in Ref. 12, there are three different values for the lattice constant c ($c_{\text{universal}} = 10 \times c_{\text{chain}} = 7 \times c_{\text{ladder}}$). Since we will mainly show the magnetic and structural properties in the chain, c_{chain} will be used to express Miller indices.

III. EXPERIMENTAL RESULTS

The temperature dependence of the magnetic susceptibility in the $\text{La}_5\text{Ca}_9\text{Cu}_{24}\text{O}_{41}$ single crystal is shown in Fig. 1(a). The susceptibility with the external field along the b axis shows a broad peak around 15 K and an abrupt decrease around 10 K. The susceptibilities with the external field along the a and c axes increase with decreasing temperature and show a tendency to saturation around 20 K. Below 20 K they increase again probably due to the Curie-Weiss tail.

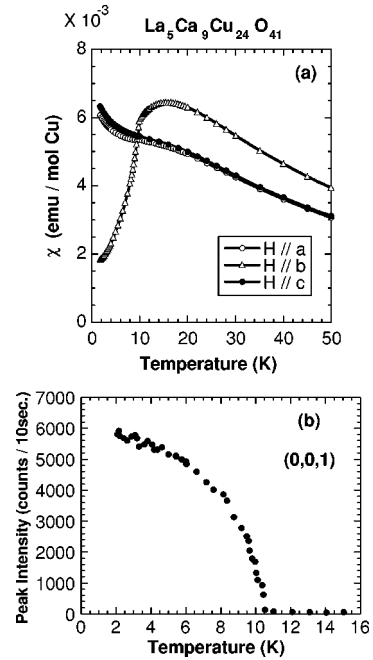


FIG. 1. (a) Temperature dependence of magnetic susceptibility in $\text{La}_5\text{Ca}_9\text{Cu}_{24}\text{O}_{41}$. (b) Temperature dependence of peak intensity at $(0,0,1)$ in $\text{La}_5\text{Ca}_9\text{Cu}_{24}\text{O}_{41}$ measured with unpolarized neutrons.

These indicate that an antiferromagnetic transition occurs around 10 K and that spins point predominantly along the b axis. The number of spins which contribute to the susceptibility is estimated from the Curie constant in the temperature range $50 \leq T \leq 250 \text{ K}$ to be $\sim 42\%$ of the total Cu^{2+} spins, which is consistent with the fact that only the chains contribute to the susceptibility below room temperature due to the large spin gap in the ladder.¹³⁻¹⁶

New Bragg reflections are observed below $\sim 10.5 \text{ K}$ at $(2n,0,1)$ (n : integer). The Bragg reflections at $(h,0,1)$ are considered to be magnetic in origin since the transition temperature corresponds to that obtained from the magnetic susceptibility measurements as mentioned above. From the positions of magnetic Bragg peaks, it is concluded that a long-range magnetic ordering occurs in the chain, which is consistent with the results of susceptibility measurements. The temperature dependence of the peak intensity at $(0,0,1)$ is shown in Fig. 1(b). Figure 2 shows an elastic scan along $[h,0,1]$ measured at 1.7 K with unpolarized neutrons. Note that a modulation of intensity is still observed along the h direction as in $\text{La}_6\text{Ca}_8\text{Cu}_{24}\text{O}_{41}$. Figure 3 shows the results of polarized neutron measurements in the vertical field. The non-spin-flip (NSF) and spin-flip (SF) mode experiments give magnetic scattering caused by spin component parallel to the field direction (b axis) and perpendicular to it, respectively. A correction originating from imperfect polarization of the neutron beam was made. Large background intensity at $(4,0,1)$ in the NSF mode comes from tail of a large nuclear Bragg reflection which originates from aluminum sample holder. The intensity observed in the SF mode was factor of ~ 20 smaller than that in the NSF mode, suggesting that only a small amount of spin component exists perpendicular to the b axis. The tilt angle from the b axis is estimated to be at most 15° . Unlike the results of the elastic neutron scan along $[h,0,1]$ in $\text{La}_6\text{Ca}_8\text{Cu}_{24}\text{O}_{41}$ where incommensurate peaks were

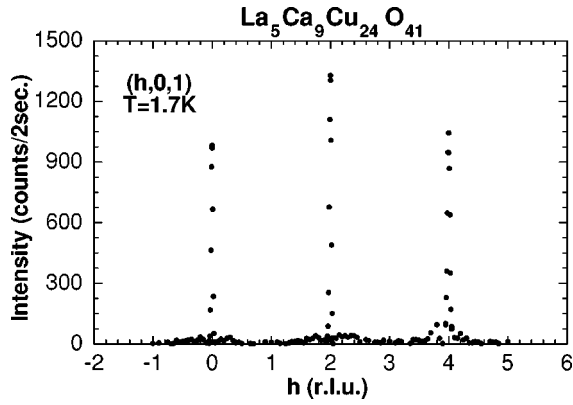


FIG. 2. An elastic neutron scan of $\text{La}_5\text{Ca}_9\text{Cu}_{24}\text{O}_{41}$ along $[h,0,1]$ measured at $T=1.7$ K with unpolarized neutrons. The data at $T=12$ K were subtracted as a background.

observed, sharp and commensurate magnetic Bragg peaks are observed in $\text{La}_5\text{Ca}_9\text{Cu}_{24}\text{O}_{41}$. From this simple diffraction pattern, a detailed magnetic structural analysis was possible in $\text{La}_5\text{Ca}_9\text{Cu}_{24}\text{O}_{41}$.

The integrated intensities of a number of magnetic peaks were obtained with unpolarized neutrons as shown in Table I. Note that the integrated intensity of magnetic Bragg peaks along $[h,0,1]$ gradually increases with increasing h . This is different from the peak height intensity which has a maximum at $h=2$ as shown in Fig. 2. This is due to the peak width increasing with increasing h because of resolution effects. In order to analyze the data, we first assume a finite c component of the Cu moment since the magnetic Bragg peak intensities in $(h,0,1)$ increase with increasing h . In this case, the spin should be tilted by $\sim 60^\circ$ from the b axis to explain the observed data. However, this model is inconsistent with our experiments since it requires that (i) the intensity in the SF mode should be large as shown by the broken lines in Fig. 3 and that (ii) the intensity of magnetic Bragg peaks along $[0,k,1]$ should have a similar Q dependence as observed along $[h,0,1]$, which is not the case.

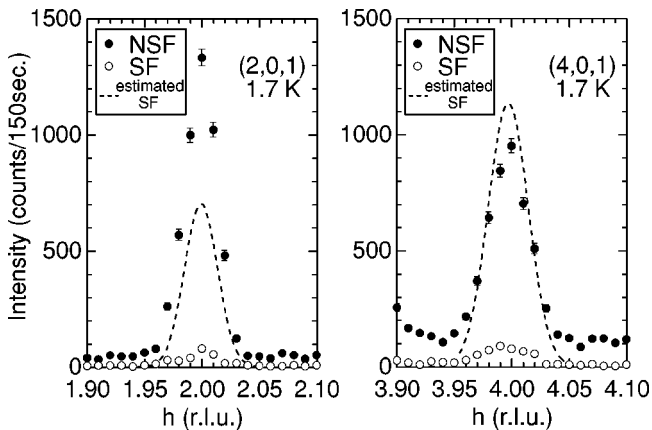


FIG. 3. Elastic neutron scans of $\text{La}_5\text{Ca}_9\text{Cu}_{24}\text{O}_{41}$ at $(2,0,1)$ and $(4,0,1)$ measured at $T=1.7$ K with polarized neutrons in the vertical field spin-flip (SF) and non-spin-flip (NSF) mode. A correction originating from imperfect polarization of the neutron beam was made. The broken lines represent scattering intensities expected when the Cu moments are tilted by 60° from the b axis as described in the text.

TABLE I. Observed integrated (I_{obs}) and calculated intensities (I_{calc}) of magnetic Bragg reflections on $\text{La}_5\text{Ca}_9\text{Cu}_{24}\text{O}_{41}$. The measurements were performed at $T=1.7$ K with unpolarized neutrons.

(h,k,l)	I_{obs}	I_{calc}
$(0,0,1)^a$	221	221
$(2,0,1)$	282	275
$(4,0,1)$	286	282
$(0,2,1)$	185	158
$(0,4,1)$	109	74
$(0,6,1)$	55	51

^aThe intensity is normalized at this reflection.

Therefore, a tilt of the Cu moments away from the chain direction cannot explain the experimental results. We now postulate that a moment induced on the oxygen sites is also present in the magnetically ordered phase. Figure 4 shows a proposed spin structure for $\text{La}_5\text{Ca}_9\text{Cu}_{24}\text{O}_{41}$. In the calculation of magnetic Bragg intensities it is assumed that a moment is induced on the oxygen sites which is parallel to the Cu spin and has a value which is 11% of the Cu moment. For the Cu^{2+} ions, the Freeman and Watson form factor calculated for the free Cu^{2+} ion was used. The same form factor was also assumed for the oxygen ions. This assumption would not affect the calculated intensities appreciably since the contribution from the oxygen is not very large. The model agrees reasonably well with the observed intensities as shown in Table I. A slight difference between observed and calculated intensities may partly come from the fact that the magnetic form factor in this compound is affected by the covalency effects as will be described in Sec. IV. The ordered Cu moment is $\sim 0.2\mu_B$ and the O moment is $\sim 0.02\mu_B$ at 1.7 K, which is estimated by normalizing the magnetic Bragg intensities with that of a weak nuclear Bragg reflection $(4,0,0)$. Because of a small number of weak nuclear Bragg

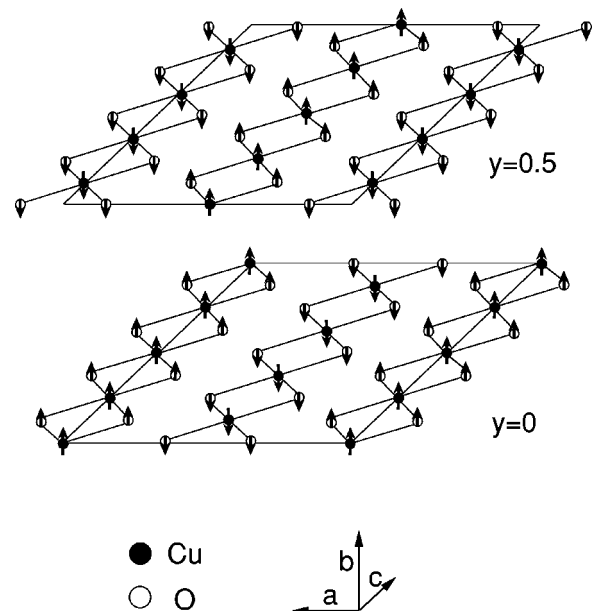


FIG. 4. A proposed model for the magnetic structure in the chain. Closed and open circles represent copper and oxygen ions, respectively.

reflections, it is difficult to determine the Cu and oxygen moments more precisely.

IV. DISCUSSION

We have clearly shown that $\text{La}_5\text{Ca}_9\text{Cu}_{24}\text{O}_{41}$ has an antiferromagnetic structure with ferromagnetic correlations along the chain direction and that the modulation of the magnetic Bragg intensities in $(h,0,1)$ along the h direction originates from induced moments at oxygen sites which couple with Cu moments ferromagnetically. From these results we can deduce the spin structure of $\text{La}_6\text{Ca}_8\text{Cu}_{24}\text{O}_{41}$. In this compound a small moment is also present on the oxygen sites since the modulation of the magnetic Bragg intensities in $(h,0,1)$ along the h direction is also observed.¹⁰ The Cu and oxygen moments probably have a conical spiral structure with a rotation of spins by $\sim 2\pi/5$ along the a axis. The tilt of the moments from the b axis is considered to be small since no distinct scattering was observed in the vertical field SF mode experiments¹¹ and the susceptibility along the b axis drops almost to zero at low temperature.¹⁰

The magnetic transition temperature in $\text{La}_5\text{Ca}_9\text{Cu}_{24}\text{O}_{41}$ (10.5 K) is lower than that in $\text{La}_6\text{Ca}_8\text{Cu}_{24}\text{O}_{41}$ (12.2 K). As mentioned above, the former is hole doped. The hole acts as a nonmagnetic impurity (Zhang-Rice singlet) which breaks the chain. It is expected that the range of magnetic correlation at low temperature is limited by the nonmagnetic sites. This would make the transition temperature lower.

It is rather difficult to understand why the magnetic structure is incommensurate in $\text{La}_6\text{Ca}_8\text{Cu}_{24}\text{O}_{41}$ which has no holes while $\text{La}_5\text{Ca}_9\text{Cu}_{24}\text{O}_{41}$ which has a small number of holes shows a commensurate structure. It is noted that the width of the magnetic Bragg peaks along the h direction is broad in $\text{La}_6\text{Ca}_8\text{Cu}_{24}\text{O}_{41}$ and resolution limited in $\text{La}_5\text{Ca}_9\text{Cu}_{24}\text{O}_{41}$. This indicates that the coupling between the chains in the former system is disturbed by some kind of disorder. A possible origin of the disorder could be excess oxygens which probably exist at interstitial sites. The excess oxygens may also cause a competition between the nearest-neighbor and next-nearest-neighbor interactions. Further study is needed to understand the origin of the spiral structure in $\text{La}_6\text{Ca}_8\text{Cu}_{24}\text{O}_{41}$.

It was also observed that the diffraction pattern in some samples of $\text{La}_6\text{Ca}_8\text{Cu}_{24}\text{O}_{41}$ consists of a superposition of the Bragg peaks of $\text{La}_5\text{Ca}_9\text{Cu}_{24}\text{O}_{41}$ ($2n,0,1$) (n : integer) and of $\text{La}_6\text{Ca}_8\text{Cu}_{24}\text{O}_{41}$ ($2n \pm \delta,0,1$) (n : integer) (Ref. 10).¹⁷ The transition temperature is ~ 14 K, which is slightly higher than in $\text{La}_6\text{Ca}_8\text{Cu}_{24}\text{O}_{41}$ as mentioned above. These are probably caused by a slight difference of La/Ca ratio or oxygen content. The superimposed diffraction pattern does not origi-

nate from inhomogeneous distribution of La and Ca in the sample since both the commensurate and incommensurate magnetic Bragg peaks show the same temperature dependence.

The strong Cu d -O p hybridization in the CuO_2 planes, in which coppers are coupled by 180° Cu-O-Cu bonds, was shown to be present in antiferromagnetic La_2CuO_4 and $\text{YBa}_2\text{Cu}_3\text{O}_{6+x}$.^{18,19} The effective copper moment is reduced due to hybridization with the oxygens. Recently, Pickett and Singh calculated the effects of Mn d -O p hybridization in the $\text{La}_{1-x}\text{Ca}_x\text{MnO}_3$ system²⁰ and showed that oxygen moments are polarized in the various magnetically ordered phases. Large covalency effects were also observed in K_2IrCl_6 (Ref. 21) and K_2CuF_4 (Ref. 22), in which magnetic form factors of Ir and Cu are affected by Ir d -Cl p and Cu d -F p hybridization, respectively. It is plausible that strong Cu d -O p hybridization also exists in edge-sharing CuO_4 chains in $\text{La}_{14-x}\text{Ca}_x\text{Cu}_{24}\text{O}_{41}$, in which coppers are coupled by ferromagnetic 90° Cu-O-Cu bonds. The interesting feature in this system is that the moments polarized at oxygen sites show an ordering. The small copper moment ($\sim 0.2\mu_B$) observed in $\text{La}_5\text{Ca}_9\text{Cu}_{24}\text{O}_{41}$ probably originates from the Cu d -O p hybridization and quantum fluctuations. Theoretical study to explain this phenomenon is highly desirable.

In conclusion, we observed that $\text{La}_5\text{Ca}_9\text{Cu}_{24}\text{O}_{41}$ shows an antiferromagnetic long-range ordering below $T_N=10.5$ K with ferromagnetic correlations in the chain. Unexpectedly, an ordering of oxygen moments ($\sim 0.02\mu_B$) is needed in addition to that of Cu moments ($\sim 0.2\mu_B$) to explain the magnetic intensities. The oxygen moments are coupled with Cu moments ferromagnetically.

ACKNOWLEDGMENTS

We would like to thank K. Katsumata, W. E. Pickett, and D.J. Singh for stimulating discussions. M.M., S.M.S., and G.S. would like to thank H. Mook, S. Nagler, and A. Tennant for their warm hospitality during their stay at Oak Ridge National Laboratory. This work was partially supported by the U.S.-Japan Cooperative Program on Neutron Scattering operated by the U.S. Department of Energy and the Japanese Ministry of Education, Science, Sports, and Culture, and by the NEDO International Joint Research Grant. Work at Brookhaven National Laboratory was carried out under Contract No. DE-AC02-76CH00016, Division of Material Science, U.S. Department of Energy. Work at Oak Ridge National Laboratory was carried out under Contract No. DE-AC05-96OR22464, Division of Material Science, U.S. Department of Energy.

*Permanent address: Department of Physics, Aoyama-Gakuin University, Chitosedai, Setagaya-ku, Tokyo 157, Japan.

¹N. Motoyama, H. Eisaki, and S. Uchida, Phys. Rev. Lett. **76**, 3212 (1996).

²K. M. Kojima, Y. Fudamoto, M. Larkin, G. M. Luke, J. Merrin, B. Nachumi, Y. J. Uemura, N. Motoyama, H. Eisaki, S. Uchida, K. Yamada, Y. Endoh, S. Hosoya, B. J. Sternlieb, and G. Shirane, Phys. Rev. Lett. **78**, 1787 (1997).

³Y. Mizuno, T. Tohyama, S. Maekawa, T. Osafune, N. Motoyama,

H. Eisaki, and S. Uchida, Phys. Rev. B **57**, 5326 (1998).

⁴M. Hase, I. Terasaki, and K. Uchinokura, Phys. Rev. Lett. **70**, 3651 (1993).

⁵A. Sapiña, J. Rodriguez-Carvajal, M. J. Sanchis, R. Ibanez, A. Beltran, and D. Beltran, Solid State Commun. **74**, 779 (1990).

⁶M. Matsuda and K. Katsumata, Phys. Rev. B **53**, 12 201 (1996).

⁷M. Matsuda, K. Katsumata, H. Eisaki, N. Motoyama, S. Uchida, S. M. Shapiro, and G. Shirane, Phys. Rev. B **54**, 12 199 (1996).

- ⁸T. Siegrist, L. F. Schneemeyer, S. A. Sunshine, J. V. Waszczak, and R. S. Roth, *Mater. Res. Bull.* **23**, 1429 (1988).
- ⁹S. A. Carter, B. Batlogg, R. J. Cava, J. J. Krajewski, W. F. Peck, Jr., and T. M. Rice, *Phys. Rev. Lett.* **77**, 1378 (1996).
- ¹⁰M. Matsuda, K. Katsumata, T. Yokoo, S. M. Shapiro, and G. Shirane, *Phys. Rev. B* **54**, 15 626 (1996).
- ¹¹M. Matsuda, K. Katsumata, T. Yokoo, S. M. Shapiro, and G. Shirane (unpublished).
- ¹²E. M. McCarron III, M. A. Subramanian, J. C. Calabrese, and R. L. Harlow, *Mater. Res. Bull.* **23**, 1355 (1988).
- ¹³M. Azuma, Z. Hiroi, M. Takano, K. Ishida, and Y. Kitaoka, *Phys. Rev. Lett.* **73**, 3463 (1994).
- ¹⁴R. S. Eccleston, M. Azuma, and M. Takano, *Phys. Rev. B* **53**, R14 721 (1996).
- ¹⁵K. Kumagai, S. Tsuji, M. Kato, and Y. Koike, *Phys. Rev. Lett.* **78**, 1992 (1997).
- ¹⁶S. Matsumoto, Y. Kitaoka, K. Magishi, K. Ishida, K. Asayama, M. Uehara, T. Nagata, and J. Akimitsu (unpublished).
- ¹⁷K. M. Kojima, Y. J. Uemura, N. Motoyama, T. Osafune, H. Eisaki, S. Uchida, and G. Shirane (private communication).
- ¹⁸T. A. Kaplan, S. D. Mahanti, and H. Chang, *Phys. Rev. B* **45**, 2565 (1992).
- ¹⁹S. Shamoto, M. Sato, J. M. Tranquada, B. J. Sternlieb, and G. Shirane, *Phys. Rev. B* **48**, 13 817 (1993).
- ²⁰W. E. Pickett and D. J. Singh, *Phys. Rev. B* **53**, 1146 (1996).
- ²¹J. W. Lynn, G. Shirane, and M. Blume, *Phys. Rev. Lett.* **37**, 154 (1976).
- ²²K. Hirakawa and H. Ikeda, *Phys. Rev. Lett.* **33**, 374 (1974).